



# The Energy and Exergy Analysis of Integrated Hydrogen Production System Using High Temperature Steam Electrolysis with Optimized Water Path

H. Raeissi Jelodar<sup>a</sup>, G. R. Salehi<sup>\*b</sup>, R. Abedini<sup>c</sup>

<sup>a</sup> Department of Energy Systems Engineering, Petroleum University of Technology, Mahmoodabad, Iran

<sup>b</sup> Department of Mechanical Engineering, Petroleum University of Technology, Abadan, Iran

<sup>c</sup> Department of Process, Faculty of Chemical Engineering, Babol Noshirvani University of Technology, Babol, Iran

## PAPER INFO

### Paper history:

Received 23 November 2018

Received in revised form 13 April 2019

Accepted 02 May 2019

### Keywords:

Solar Driven Integrated System

Hydrogen Production

High-temperature Steam

Electrolysis

Thermodynamic Analysis

Energy

## ABSTRACT

In this research, solar-driven integrated Hydrogen production (HP) using high-temperature steam electrolysis (HTSE) is thermodynamically evaluated. This system includes an organic Rankine cycle (ORC), Rankine cycle, Brayton cycle, solar tower, and High Temperature Steam Electrolysis (HTSE). Solar energy supplies thermal energy. This heat source is applied for generating power. This energy is used for HTSE due to its demand in the form of electricity. First, we calculated inlet and outlet energy and their rates for whole subsystems. The results showed 50.77% overall and 31.63% exergy efficiencies related to power generation section and 92.85% overall energy and 91% exergy efficiencies related to hydrogen production section. Also in this research we found the importance of auxiliary equipment. Auxiliary equipment helps that significant amount of hydrogen production to be saved. This amount at 577 K is equal that produces 0.093 kg H<sub>2</sub>/s

doi: 10.5829/ije.2019.32.06c.14

## NOMENCLATURE

$\dot{m}$	Mass flow rate, kg/s	NOH	Number of heliostats
h	Enthalpy, kJ/kg	TAOH	Total area of heliostats, m <sup>2</sup>
P	Pressure, kPa	WF	Working fluid
T	Temperature, K	CR <sub>Br</sub>	Compression ratio
C <sub>p</sub>	Constant pressure	TPC	Turbine power capacity
C <sub>v</sub>	Constant volume	TIT	Turbine inlet temperature
k	Special heats coefficient	TEP	Turbine exit pressure
LHV	Low heating value, kJ/kg	$\dot{E}_x^Q$	Exergy due to heat transfer
y <sub>i</sub>	Mole fraction	$\dot{E}_x^W$	Exergy from work

## 1. INTRODUCTION

The world's dependence on fossil fuels to supply energy to industries, transportation sectors, power generation and buildings has sharply increased since the industrial revolution. Indeed, the life standards have increased as well as energy consumption and the use of renewable energy is very important in replacement of fossil fuels [1]. However, some concern such as, climate change, global warming, acid rains, pollution, melting of ice

caps, sea levels increasing and ozone layer depletion caused by excess utilization of fossil fuel in different approaches [2] and alternative energies became much more important [3]. Hydrogen has been considered by researchers as an alternative renewable and clean energy resource in different approaches, from methanol production [4] to pure and or fuel additive in internal combustion engines [5]. Although hydrogen abundantly exists in the earth, it is just found in composition of other materials [6]. In consequent, hydrogen production (HP) is now one of the most interesting field of study and extended works were conducted to improve its

\*Corresponding Author Email: rezasalehi20@gmail.com (G. R. Salehi)



**TABLE 1.** General characteristics of the proposed system

<b>Solar tower</b>	
RH	65 m
NOH	69
TAOH	8349 m <sup>2</sup>
<b>Brayton Cycle</b>	
WF	Air
$\eta_{rr}$	0.92
$\eta_{ic}$	0.88
$CR_{Br}$	11.2
TPC	5670 kW
<b>Rankine Cycle</b>	
WF	Water
$\eta_{rr}$	0.91
$\eta_{ip}$	0.88
TIT	623.15 K
TIP	3000 kPa
TEP	65 kPa
TPC	1020 kW
ORC	
WF	CO <sub>2</sub>
$\eta_{rr}$	0.95
$\eta_{ip}$	0.90
TIT	453.15 K
TIP	15000 kPa
TEP	7000 kPa
TPC	445 kW

Quero et al. [17] investigated a receiver that was mounted at the top of the tower at an altitude of 65 meters and the space of the heliostat is 8350m<sup>2</sup>. Initially, the compressed air in the solar tower receiver is heated to 1078.15K and then enters to the combustion chamber. Natural gas is used for the combustion process, and the air heats up to its final temperature before entering the gas turbine. gas turbine selected model is Taurus model from solar Turbines [17, 24]. It has a compression ratio of 11.2, with a capacity of 5670 kW. The main advantage of gas turbine is its compact design. The exhaust gases from the turbine then pass through three heat exchangers to supply heat-to-water supply for the HP process, the Rankin cycle and the transferring ORC. The Rankin cycle works with water as a liquid and has a capacity of 1020 kW. The last ORC cycle that works as a fluid. ORC is a method of using low temperature heat; Energy transformation technology is promising and can

increase energy by converting heat into electrical energy. In the system, the R744 fluid is pumped from the condenser using a liquid pump and its thermal energy is received from the heat exchanger and liquid switched to superheated steam. The superheated steam then enters the turbine and expands to low pressure. At the outlet of the ORC turbine, the R744 steam enters to recuperator for preheating of the R744 after pumping process. Subsequently, the turbine exhaust is exacerbated by a cooling tower for extraction of heat into the liquid medium at the condenser. The general properties of the solar energy system are presented in Figure 1. To analyze the proposed system performance, the energy and exergy equations of each cycle components should be separately applied. In this section, the required equations are introduced. To simplify the modeling, the following assumptions are used:

- All sections (Brayton cycle, Rankine cycle, ORC, and electrolyser) are Steady State Steady Flow (SSSF) process.
- Air and combustion products considered as ideal gases.
- Methane used as fuel in the combustion chamber.
- Condensers outflow considered as saturated liquid in the Rankine and ORC cycle.
- The properties of CO<sub>2</sub> and water are Compatible from thermodynamic tables.

### 3. ENERGY ANALYSIS

Given the assumption mentioned to describe the mathematical model, the energy equation and mass conservation law for each component as SSSF process [25].

$$\sum \dot{m}_e = \sum \dot{m}_i \quad (1)$$

$$\dot{Q} - \dot{W} = \sum \dot{m}_e h_e - \sum \dot{m}_i h_i \quad (2)$$

where, h and  $\dot{m}$  refer to the enthalpy and mass flow rate, respectively. Also, subscripts e and i refer to exhaust and inlet conditions.

Generating power of three cycle is the total power generated and consumed by compressors, turbines and pumps. The thermal efficiency is the ratio of production to the heat of the input. For example, in the brayton cycle:

$$\dot{W}_{net} = \dot{W}_{GT} + \dot{W}_{comp1} + \dot{W}_{comp2} \quad (3)$$

$$\dot{Q}_{net} = \dot{Q}_{receiver} + \dot{Q}_{C.Ch} \quad (4)$$

$$\eta_I = \frac{\dot{W}_{net}}{\dot{Q}_{net}} \quad (5)$$

The mass flow rate required for fuel consumption, the ORC and Rankin cycle, and the HP supply feedwater are calculated from the temperature gradient generated on the hot side of the heat exchangers. Assuming the heat exchangers are insulated, we must have:

$$\dot{m}_{air}C_p(T_6 - T_5) = \dot{m}_{fuel}\eta_{comb}LHV \quad (6)$$

$$\dot{m}_{air}C_p(T_8 - T_7) = \dot{m}_{water}(h_{22} - h_{23}) \quad (7)$$

$$\dot{m}_{air}C_p(T_9 - T_8) = \dot{m}_{Rankine}(h_{12} - h_{13}) \quad (8)$$

$$\dot{m}_{air}C_p(T_{10} - T_9) = \dot{m}_{Rankine}(h_{17} - h_{18}) \quad (9)$$

where, LHV and  $\eta_{comb}$  are the low heating value of fuel and combustion efficiency, respectively; which are considered by 0.98 and 47.13 MJ/kg [26].

#### 4. EXERGY ANALYSIS

Analysis of the second law of each component is possible after applying the first law and calculating the thermodynamic properties of the fluid. To achieve this, the exergy equilibrium is used, for example:

$$\dot{E}x^Q + \sum \dot{m}_i ex_i = \dot{E}x^W + \sum \dot{m}_e ex_e + I \quad (10)$$

where,  $ex$ ,  $\dot{E}x^W$ ,  $\dot{E}x^Q$  and  $I$  refer to exergy due to exergy destruction, exergy from work, specific exergy and heat transfer, respectively. Total exergy consists of chemical and thermo-mechanical exergy and is stated as follows:

$$ex = ex_{tm} + ex_{ch} \quad (11)$$

$$ex_{tm} = (h - h_0) - T_0(s - s_0) \quad (12)$$

$$ex_{ch} = \sum_{i=1}^N y_i ex_i^{ch} + RT_0 \sum_{i=1}^N y_i \ln(y_i) \quad (13)$$

$y_i$  refers to the mole fraction of flu composition.  $s$  Refers to entropy and index 0 refers to the dead state, working fluids in ambient pressure and temperature. The fuel exergy is also calculated from the semi-empirical equation [27]:

$$\epsilon = \frac{ex_{fuel}}{LHV_{fuel}} \quad (14)$$

The value of  $\epsilon$  is close to the unit. Exergy transmission due to work and heat through the borders is:

$$\dot{E}x^W = \dot{W} \quad (15)$$

$$\dot{E}x^Q = \left(1 - \frac{T_0}{T_s}\right) \dot{Q} \quad (16)$$

where,  $T_s$  is the source temperature. The effectiveness of the second law as a more precise criterion for the functioning of the system is defined, as the division of exergy to the consume one:

$$\eta_{II} = \frac{Ex_{net}}{Ex_i - Ex_e} \quad (17)$$

For HP performance analysis, first law efficiency is defined as the ratio of LHV of separated hydrogen from feed water to heat entered to the system. For second law efficiency, separated hydrogen exergy is compared via inlet exergy:

$$\eta_I = \frac{\dot{m}_{H_2,sep} * LHV_{H_2}}{Q_{in}} \quad (18)$$

$$\eta_{II} = \frac{Ex_{H_2,sep}}{Ex_{in}} \quad (19)$$

## 5. RESULTS AND DISCUSSION

**5. 1. Validation** The integrated solar system for sustainable HP was investigated via HTSE method. The system was analyzed based on the model and hypotheses. In this analysis, we examine the system using the governing equations of total mass, energy, and exergy. For analyzing and applying thermodynamic equations at a temperature of 25°C and a pressure of 101kPa, EES software was used. The proposed cycle in this research is a new idea. Therefore, there are no experimental data for validating the model results. So, each cycle is confirmed separately with the previous study [17] as reported in Table 2. Since the accuracy of the model is within the acceptable range, it can be stated that the results from the production model are reliable.

**5. 2. Results of Analysis** The thermodynamic characteristics of the fluid in each vapor reported in Table 3. Using these data and the equations defined in the description section of the model is defined, the system performance is summarized in Table 4.

The power generation capacity of the Brayton, Rankine and ORC cycles was reported in Table1. As a result, the total electricity generated by three cycles for the production of hydrogen is 8873 kW. According to the analysis, Brayton cycle efficiency was 43.1% while the efficiency of the Rankine cycle was 24.23% and the ORC cycle was 19.81%. For the analysis of the second

**TABLE 2.** Validation of simulation data

cycle	energy efficiency		exergy efficiency		$\frac{\dot{m}_{H_2,prod.}}{\dot{m}_{H_2,int.}} \%$	
	ref [17]	Sim.	ref [17]	Sim.	ref [17]	Sim.
Brayton	38.7	38.5	47.7	50.7	-	-
Rankine	24.2	24.2	40.1	63.7	-	-
ORC	25.2	25.2	40.5	32.5	-	-
Simple PGS	24.7	24.6	22.3	27.1	-	-
Simple HTSE	-	30.9	-	0.39	66.6	65.4

**TABLE 3.** each steam characteristics of proposed system

State NO	fluid	$T$ [K]	$P$ [kPa]	$\dot{m}$ [kg/s]	$h$ [kJ/kg]
1	Air	298.2	101.3	14.24	298.6
2	Air	434.9	339	14.24	436.4
3	Air	298.2	1135	14.24	298.6
4	Air	434.9	135	14.24	436.7
5	Air	903.6	1135	14.24	937.2
6	Air	1523	101.3	14.24	1664
7	Air	833.2	101.3	14.24	858.9
8	Air	795.4	101.3	14.24	777.8
9	Air	1023	101.3	14.24	1072
10	Air	1101	65	14.24	1163
11	$H_2O$	361.1	30000	1.528	368.5
12	$H_2O$	361.4	3000	1.528	371.9
13	$H_2O$	623.2	65	1.528	3115
14	$H_2O$	361.1	7000	1.528	2447
15	$CO_2$	301.8	15000	9.221	-213.9
16	$CO_2$	320.4	15000	9.221	-201.1
17	$CO_2$	367.1	15000	9.221	-58.1
18	$CO_2$	453.1	7000	9.221	81.55
19	$CO_2$	383.4	7000	9.221	33.3
20	$CO_2$	303.7	101.1	9.221	109.7
21	$H_2O$	298.2	101.1	0.85	104.8
22	$H_2O$	373.1	101.1	0.85	2418
23	$H_2O$	905.1	101.1	0.85	3776
24	$H_2O$	905.1	101.1	0.28	3776
25	$H_2O$	1185	101.1	0.28	4426
26	$H_2O$	905.1	101.1	0.57	3776
27	$H_2O$	1185	101.1	0.57	4426
28	$H_2O$	1185	101.1	0.85	4426
29	$H_2$	1233	10000	0.093	12881
30	$O_2$	1233	10000	0.7464	966.3
31	$O_2$	569	7000	0.7464	258.14
32	$H_2$	577	7000	0.093	3913

law, the exergy efficiency of Brayton, Rankine and ORC cycles has been reported to be 57.42, 46.41 and 45.72%, respectively. The exergy rate of destruction for three Brayton, Rankine and ORC cycles is 29700, 616.6 and 325.4 kW, respectively. Also, the exergy rate for

**TABLE 4.** proposed system performance

Parameter	Value
Net power	8873 kW
Net irreversibility	32.65 kW
consumed fuel	1.14 kg/s
Produced $H_2$	0.09 kg/s
$\eta_{I,PGS}$	50.7 %
$\eta_{I,H_2}$	98.3 %

system PG degradation is 30642 kW. The overall exergy and energy efficiency of the PGS is 31.63 and 50.77%, respectively. For the HTSE hydrogen production section, energy and exergy efficiency results are 92.85 and 91.01%, respectively, which is higher than the previous HTSE hydrogen production models. Increasing the efficiency due to the change in the direction of the inlet water into the electrolyser, causes an increase of inlet steam temperature. The results showed that without the auxiliary facilities, the hydrogen produced at a temperature of 577K is 0.093kg/s. This amount of hydrogen compared to the amount of hydrogen produced in previous studies of hydrogen production by HTSE method has a remarkable advantage.

The effects of the temperature and pressure inlets on the turbine of the Brayton cycle have been specifically analyzed from the PG section. To determine the effect of system parameters on exergy degradation, system power and energy efficiency in Brayton cycle and the PG section as well as the hydrogen production efficiency for a specific case, we study the results of the, Brayton cycle by changing the pressure and temperature. Upon increasing turbine inlet temperatures from 1,400 to 1,600 K, turbine power increases, which increases energy efficiency, exergy and exergy degradation. However, an increase in the exergy increase in exhaust emissions is less than the energy efficiency and exergy.

Proposed system performance due to the change of Brayton turbine inlet temperature, when the other inlet parameters were considered to be constant, are shown in Figure 2. Demanded Figure 3 proposed system performance due to the change of Brayton turbine inlet temperature. Fuel was increased 36.8% to achieve 1600 K, while the heat received from the sun had no change. Consumed fuel enhancement rate was greater than turbine out power one, so the ratio of powers to added heat in combustion chamber was slightly decreased. Furthermore, the irreversibility of general system was increased due to the more temperature of heat transfer in heat exchangers and hydrogen production efficiency was decreased by 6% due to the fuel consumption

increase caused by turbine inlet temperature enhancement. System response to input heat flux from the sun is shown in Figure 3 and considering fixed turbine inlet temperature, less fuel is needed when the input heat flux was increased. Consequently, the ratio of produced power and hydrogen to consumed heat in combustion chamber were increased by 29 and 13%, respectively. Produced power and efficiency of Brayton cycle are affected by compression ratio and to investigate its effect on system performance it was changed between 810 and 1600 kPa. In Figure 4, first and second law efficiencies, produced power and irreversibility of Brayton cycle via compression ratio changes were shown. All of them were increased by compression ratio enhancement due to more turbine power generation rate than compressor power consumption rate. Irreversibility was also increased due to the enhancement of mean working pressure of cycle. Considering Brayton cycle as the main PG core of PGS, total power was increased as well as Brayton cycle.

To investigate the role of working fluid on ORC performance, its energy and exergy parameters are compared employing two different working fluids namely, carbon dioxide (R744) and ammonia (R717) which are shown in Figure 5. In case of using carbon dioxide as working fluid, less net power was achieved and irreversibility decreased noticeably. The interaction of less power and irreversibility caused both more energy and exergy efficiencies when carbon dioxide employed as working fluid.

The total amount of energy received, the process of hydrogen production and power generation is 17467 kW. This amount of energy comes from solar energy and burning natural gas in the combustion chamber. The energy used to run two Rankin, ORC, and also Electrolyzer devices. Respectively, the energy required for the ORC cycle, the Rankin and the Electrolyzer is 1288, 4191, and 1154 kW, respectively. The amount of 1334.3 kW of energy from point 10 enters the environment, which is suitable for heat stove design (Figure 6).

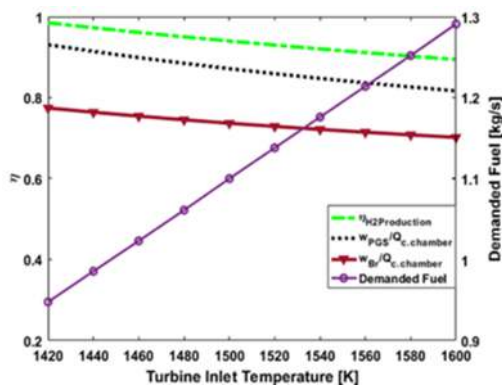


Figure 2. First law analysis of proposed system via turbine inlet temperature

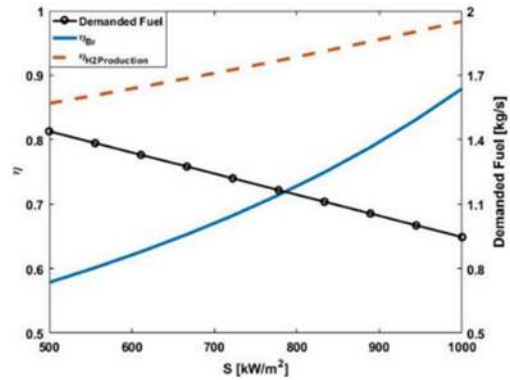


Figure 3. First law analysis of proposed system via sun heat flux

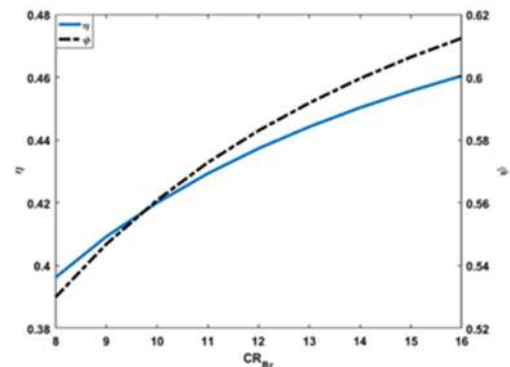


Figure 4. First and second law efficiencies of Brayton cycle

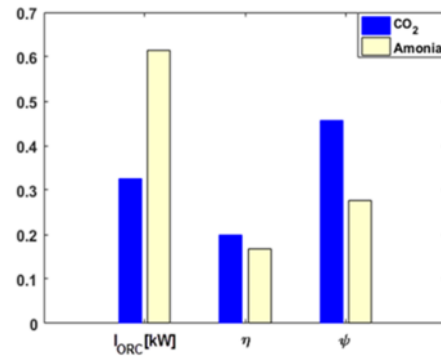


Figure 5. Irreversibility, energy and exergy efficiencies of ORC via ORC working fluid

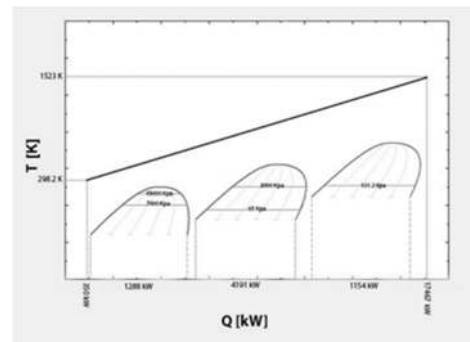


Figure 6. The amount of energy received by the cycle ORC, Rankin and electrolyzer is generated from the total energy

## 6. CONCLUSION

In this research we compared production of sustainable hydrogen with HP by HTSE thermodynamically. Here we use this electrolysis system for producing hydrogen. This system need heat energy. In order to this demand, the applied power generation system supply heat energy by producing electricity and exhaust gases the total electricity generated by three cycles for the production of hydrogen is 8873kW. In order to achieve our objective, we calculated system efficiencies and rates of exergy destruction by analyzing system's energy and exergy. Results showed that in power generation system including solar tower, the total rate of exergy destruction is equal to 30642kW. The main factor of this result was tower system because of heliostat field area's number and transfer process. Also, the efficiency of total energy for PGS was 50.77% while it was 92.85 for hydrogen production and the efficiency of total exergy for power generation was 31.63% while it was 92.85% for hydrogen production. Moreover, we analyzed system performance parametrically and also we obtained 0.093 kg H<sub>2</sub>/s. Our research should investigate problems more about maintaining greener energy. Finally, we suggest that in future studies, it's better to focus on progressing, installing and modeling about systems of sustainable hydrogen production.

## 7. REFERENCES

- Jafaryar M., R. Kamrani, M. Gorji-Bandpy, M. Hatami, and D. D. Ganji, "Numerical optimization of the asymmetric blades mounted on a vertical axis cross-flow wind turbine," *International Communications in Heat and Mass Transfer*, Vol. 70 (2016), 93-104.
- I. Dincer, "Renewable energy and sustainable development: a crucial review," *Renewable Sustainable Energy Reviews*, Vol. 4, No. 2, (2000) 157-175.
- Yilanci, A., Dincer, I. and Ozturk; H. K. "A review on solar-hydrogen/fuel cell hybrid energy systems for stationary applications." *Progress in Energy and Combustion Science* 35, No. 3 (2009): 231-244.
- J.-I. Yang, T. W. Kim, J. C. Park, T.-H. Lim, H. Jung, and D. H. Chun, "Development of a stand-alone steam methane reformer for on-site hydrogen production," *International Journal of Hydrogen Energy*, Vol. 41, No. 19, (2016) 8176-8183.
- P. Colbertaldo, G. Guandalini, and S. Campanari, "Modelling the integrated power and transport energy system: The role of power-to-gas and hydrogen in long-term scenarios for Italy," *Energy*, Vol. 154, (2018) 592-601.
- M. Sheikholeslami, "Magnetic field influence on CuO-H<sub>2</sub>O nanofluid convective flow in a permeable cavity considering various shapes for nanoparticles," *International Journal of Hydrogen Energy*, Vol. 42, No. 31, (2017) 19611-19621.
- S., Safari sabet, M.M., Namar, M., Sheikholeslami, A. Shafee., "Thermodynamics analysis for high temperature hydrogen production system", *Scientia Iranica*, 2019. doi: 10.24200/sci.2019.52022.2487.
- M.M., Namar, and O., Jahanian, Energy and exergy analysis of a hydrogen-fueled HCCI engine. *Journal of Thermal Analysis and Calorimetry*, 2018. <https://doi.org/10.1007/s10973-018-7910-7>.
- X. Zhang, J. E. O'Brien, G. Tao, C. Zhou, and G. K. Housley, "Experimental design, operation, and results of a 4 kW high temperature steam electrolysis experiment," *Journal of Power Sources*, Vol. 297, (2015) 90-97.
- J. Udagawa, P. Aguiar, and N. P. Brandon, "Hydrogen production through steam electrolysis: Model-based steady state performance of a cathode-supported intermediate temperature solid oxide electrolysis cell," *Journal of Power Sources*, Vol. 166, No. 1, (2007) 127-136.
- A. Demin, E. Gorbova, and P. Tsiakaras, "High temperature electrolyzer based on solid oxide co-ionic electrolyte: A theoretical model," *Journal of Power Sources*, Vol. 171, No. 1, (2007) 205-211.
- A. Bilodeau and K. Agbossou, "Control analysis of renewable energy system with hydrogen storage for residential applications," *Journal of Power Sources*, Vol. 162, No. 2, (2006) 757-764.
- M. Nouri, M. M. Namar, and O. Jahanian, "Analysis of a developed Brayton cycled CHP system using ORC and CAES based on first and second law of thermodynamics," *Journal of Thermal Analysis and Calorimetry*, Vol. 135, No. 3 (2019), 1743-1752.
- B. Yildiz and M. S. Kazimi, "Efficiency of hydrogen production systems using alternative nuclear energy technologies," *International Journal of Hydrogen Energy*, Vol. 31, No. 1, (2006) 77-92.
- J. Sigurvinsson, C. Mansilla, P. Lovera, and F. Werkoff, "Can high temperature steam electrolysis function with geothermal heat?," *International Journal of Hydrogen Energy*, Vol. 32, No. 9, (2007) 1174-1182.
- H. Ozcan and I. Dincer, "Energy and exergy analyses of a solar driven MgeCl hybrid thermochemical cycle for co-production of power and hydrogen," *International Journal of Hydrogen Energy*, Vol. 39, No. 15330, (2014).e41.
- M. T. Balta, O. Kizilkan, and F. Yilmaz, "Energy and exergy analyses of integrated hydrogen production system using high temperature steam electrolysis," *International Journal of Hydrogen Energy*, Vol. 41, No. 19, (2016) 8032-8041.
- H. Jokar and A. Tavakolpour-Saleh, "A novel solar-powered active low temperature differential Stirling pump," *Renewable Energy*, Vol. 81, (2015) 319-337.
- A. R. Tavakolpour, A. Zomorodian, and A. A. Golneshan, "Simulation, construction and testing of a two-cylinder solar Stirling engine powered by a flat-plate solar collector without regenerator," *Renewable Energy*, Vol. 33, (2008) 77-87.
- Zare, S.H., Tavakolpour-Saleh, A.R.: Nonlinear dynamic analysis of solar free piston hot-air engine. *Modares Mechanical Engineering*, 15, No. 9 (2015), 223-234.
- H. Karabulut, "Dynamic analysis of a free piston Stirling engine working with closed and open thermodynamic cycles," *Renewable Energy*, Vol. 36, (2011) 1704-1709.
- J. Sigurvinsson, Jon, Christine Mansilla, B. Armason, André Bontemps, Alain Maréchal, T. I. Sigfusson, and F. Werkoff. , "Heat transfer problems for the production of hydrogen from geothermal energy," *Energy conversion and management*, Vol. 47, No. 20, (2006) 3543-3551.
- A. S. Joshi, I. Dincer, and B. V Reddy, "Exergetic assessment of solar hydrogen production methods," *International Journal of Hydrogen Energy*, Vol. 35, No. 10, (2010) 4901-4908.
- H. Nami and E. Akrami, "Analysis of a gas turbine based hybrid system by utilizing energy, exergy and exergoeconomic methodologies for steam, power and hydrogen production,"



- Energy Conversion and Management*, Vol. 143, (2017) 326–337.
25. R. E. Sonntag, C. Borgnakke, G. J. Van Wylen, and S. Van Wyk, *Fundamentals of Thermodynamics*, Vol. 6. Wiley New York, (1998).
26. M. M. Namar and O. Jahanian, "A simple algebraic model for predicting HCCI auto-ignition timing according to control oriented models requirements," *Energy Conversion Management*, Vol. 154, pp. 38–45, 2017.
27. A. Mohammadi, M. H. Ahmadi, M. Bidi, F. Joda, A. Valero, and S. Uson, "Exergy analysis of a Combined Cooling, Heating and Power system integrated with wind turbine and compressed air energy storage system," *Energy Conversion Management*, Vol. 131, (2017) 69–78.

## The Energy and Exergy Analysis of Integrated Hydrogen Production System Using High Temperature Steam Electrolysis with Optimized Water Path RESEARCH NOTE

H. Raeissi Jelodar<sup>a</sup>, G. R. Salehi<sup>b</sup>, R. Abedini<sup>c</sup>

<sup>a</sup> Department of Energy Systems Engineering, Petroleum University of Technology, Mahmoodabad, Iran

<sup>b</sup> Department of Mechanical Engineering, Petroleum University of Technology, Abadan, Iran

<sup>c</sup> Department of Process, Faculty of Chemical Engineering, Babol Noshirvani University of Technology, Babol, Iran

### P A P E R I N F O

### چکیده

#### Paper history:

Received 23 November 2018  
Received in revised form 13 April 2019  
Accepted 02 May 2019

#### Keywords:

Solar Driven Integrated System  
Hydrogen Production  
High-temperature Steam  
Electrolysis  
Thermodynamic Analysis Energy

در این تحقیق، تولید هیدروژن مجتمع شده با انرژی خورشیدی (HP) با استفاده از الکترولیز بخار با درجه حرارت بالا (HTSE)، ارزیابی ترمودینامیکی می شود. این سیستم شامل یک چرخه رانکین آلی (ORC)، چرخه رانکین، چرخه ی برایتون، برج خورشیدی و الکترولیز بخار با درجه حرارت بالا (HTSE) می باشد. انرژی خورشیدی تامین کننده انرژی حرارتی می باشد. این انرژی حرارتی برای تولید نیرو اعمال می شود. این انرژی به دلیل تقاضای آن به شکل برق مورد استفاده قرار می گیرد. اول، ما انرژی ورودی و خروجی و نرخ های آنها را برای زیر سیستم های کل محاسبه کرد. نتایج به دست آمده حاوی ۵۰٫۷۷٪ کل انرژی و ۳۱٫۶۳٪ بهره وری از انرژی مربوط به بخش تولید برق و ۹۲٫۸۵٪ انرژی کلی و ۹۱٫۰۱٪ بهره وری از انرژی مربوط به بخش تولید هیدروژن است. همچنین در این تحقیق ما اهمیت تجهیزات کمکی را در بر داشتیم. تجهیزات کمکی کمکی می کند که مقدار قابل توجهی تولید هیدروژن ذخیره شود. این مقدار برابر با ۵۷۷ کیلوگرم است که ۰٫۰۳ کیلوگرم بر ثانیه H<sub>2</sub> تولید می کند.

doi: 10.5829/ije.2019.32.06c.14